



# Susceptibility to neurofibrillary tangles: role of the PTPRD locus and limited pleiotropy with other neuropathologies

## Citation

Chibnik, L. B., C. C. White, S. Mukherjee, T. Raj, L. Yu, E. B. Larson, T. J. Montine, et al. 2017. "Susceptibility to neurofibrillary tangles: role of the PTPRD locus and limited pleiotropy with other neuropathologies." *Molecular psychiatry* :10.1038/mp.2017.20. doi:10.1038/mp.2017.20. <http://dx.doi.org/10.1038/mp.2017.20>.

## Published Version

doi:10.1038/mp.2017.20

## Permanent link

<http://nrs.harvard.edu/urn-3:HUL.InstRepos:34492045>

## Terms of Use

This article was downloaded from Harvard University's DASH repository, and is made available under the terms and conditions applicable to Other Posted Material, as set forth at <http://nrs.harvard.edu/urn-3:HUL.InstRepos:dash.current.terms-of-use#LAA>

## Share Your Story

The Harvard community has made this article openly available.  
Please share how this access benefits you. [Submit a story](#).

[Accessibility](#)



## Susceptibility to neurofibrillary tangles: role of the *PTPRD* locus and limited pleiotropy with other neuropathologies

Lori B Chibnik, PhD, MPH<sup>1,2,3,4</sup>, Charles C White, PhD<sup>1,3</sup>, Shubhabrata Mukherjee, PhD<sup>5</sup>, Towfique Raj, PhD<sup>1,3</sup>, Lei Yu, PhD<sup>6</sup>, Eric B. Larson, MD, MPH<sup>7</sup>, Thomas J. Montine, MD, PhD<sup>8</sup>, C. Dirk Keene, MD, PhD<sup>8</sup>, Joshua Sonnen, MD<sup>9</sup>, Julie A. Schneider, MD<sup>6</sup>, Paul K. Crane, MD, MPH<sup>5</sup>, Joshua M. Shulman, MD, PhD<sup>10,11</sup>, David A Bennett, MD<sup>7,#</sup>, and Philip L De Jager, MD, PhD<sup>1,2,3,\*,#</sup>

<sup>1</sup>Program in Translational NeuroPsychiatric Genomics, Institute for the Neurosciences, Departments of Neurology & Psychiatry, Brigham and Women's Hospital, Boston, MA 02115, USA

<sup>2</sup>Department of Neurology, Harvard Medical School, Boston, MA, 02115, USA

<sup>3</sup>Medical and Population Genetics, Broad Institute of MIT and Harvard, Cambridge, MA, 02142, USA

<sup>4</sup>Department of Epidemiology, Harvard T.H. Chan School of Public Health, Boston, MA, 02115, USA

<sup>5</sup>Department of Medicine, University of Washington, Seattle, WA 98104, USA

<sup>6</sup>Rush Alzheimer's Disease Center, Rush University Medical Center, Chicago, IL 60612, USA

<sup>7</sup>Group Health Research Institute, Seattle, WA 98101, USA

<sup>8</sup>Department of Pathology, University of Washington, Seattle, WA, USA

<sup>9</sup>Department of Pathology, University of Utah, Salt Lake City, UT

<sup>10</sup>Departments of Neurology, Molecular and Human Genetics, Neuroscience and Program in Developmental Biology, Baylor College of Medicine, Houston, TX 77030, USA

<sup>11</sup>Jan and Dan Duncan Neurological Research Institute, Texas Children's Hospital, Houston, TX 77030, USA

Users may view, print, copy, and download text and data-mine the content in such documents, for the purposes of academic research, subject always to the full Conditions of use: [http://www.nature.com/authors/editorial\\_policies/license.html#terms](http://www.nature.com/authors/editorial_policies/license.html#terms)

\*Correspondence: Philip L. De Jager, MD, PhD, Program in Translational NeuroPsychiatric Genomics, Departments of Neurology & Psychiatry, Brigham and Women's Hospital, 77 Avenue Louis Pasteur, NRB 168C, Boston, MA 02115, Phone: 617 525-4529, Fax: 617 525-5333, [pdejager@rics.bwh.harvard.edu](mailto:pdejager@rics.bwh.harvard.edu).

#Contributed equally

### Conflict of Interest:

Dr. Schneider is a consultant for Navidea Biopharmaceuticals and an advisor to Eli Lilly Inc. and Genetech. All other authors report no conflict of interest.

**AUTHOR CONTRIBUTIONS:** C.D.K., J.S., and J.A.S. collected, prepared and generated data from the samples. L.B.C., C.C.W., T.R. and L.Y. performed analyses on the resulting data. S.M., E.B.L., T.J.M., C.D.K., J.S., and P.K.C. generated and analyzed the replication data. E.B.L., T.J.M. and P.K.C. designed the replication study. P.L.D. and D.A.B. designed the primary study. P.L.D., C.C.W., J.M.S. and L.B.C. wrote the manuscript. All of the authors critically reviewed the manuscript.

## Abstract

Tauopathies, including Alzheimer's disease (AD) and other neurodegenerative conditions, are defined by a pathological hallmark: neurofibrillary tangles (NFT). NFT accumulation is thought to be closely linked to cognitive decline in AD. Here, we perform a genome-wide association study for NFT pathologic burden and report the association of the *PTPRD* locus (rs560380,  $p=3.8 \times 10^{-8}$ ) in 909 prospective autopsies. The association is replicated in an independent dataset of 369 autopsies. The association of *PTPRD* with NFT is not dependent on the accumulation of amyloid pathology. In contrast, we find that the *ZCWPW1* AD susceptibility variant influences NFT accumulation and that this effect is mediated by an accumulation of amyloid  $\beta$  plaques. We also performed complementary analyses to identify common pathways that influence multiple neuropathologies which co-exist with NFT and found suggestive evidence that certain loci may influence multiple different neuropathological traits, including tau, amyloid  $\beta$  plaques, vascular injury and Lewy bodies. Overall, these analyses offer an evaluation of genetic susceptibility to NFT, a common endpoint for multiple different pathologic processes.

Multiple neurologic diseases can lead to loss of cognitive function with older age. Several of them can be grouped by neuropathologic changes found at autopsy, such as neurofibrillary degeneration which is best characterized by the accumulation of neurofibrillary tangles (NFT). "Tauopathies" share the accumulation of aggregates consisting of the Microtubule Associated Protein Tau (Tau) but have different clinical manifestations and distinct etiologies that ultimately converge in the abnormal accumulation of Tau species. Tauopathies include such neurodegenerative disorders as Alzheimer's disease (AD), some forms of frontotemporal degeneration, progressive supranuclear palsy, cortico-basal degeneration, as well as forms of neurodegeneration occurring secondary to environmental insults, such as in chronic traumatic encephalopathy<sup>1</sup>. In an older population, it is possible that multiple different disease mechanisms interact to lead to the accumulation of NFT. Identifying risk factors that contribute to the accumulation of pathologic Tau is therefore meaningful, not just for the vast majority of the population that is at risk for AD but even more broadly for informing our understanding of other tauopathies.

Here, we leverage neuropathologic data collected from two longitudinal cohorts of aging whose participants are non-demented at the time of enrollment; in both the Religious Order Study (ROS) and the Rush Memory and Aging Project (MAP), brain donation is a condition of enrollment. Importantly, these subjects represent a sample of the older population in which multiple different neuropathologic changes are present, including NFT but also amyloid  $\beta$  plaques, vascular injury, Lewy bodies, and other pathologic changes. We focused on factors that influence NFT accumulation from all central nervous system insults commonly experienced by older subjects. Thus, in our discovery study, we performed a quantitative trait analysis to identify susceptibility loci for NFT and replicated our main result in an independent longitudinal cohort of aging with neuropathologic data.

In individuals selected as AD cases or AD controls, a recent genome-wide association study (GWAS)<sup>2</sup> sought genetic factors associated with multiple individual neuropathologies, using correlations in beta estimates to discuss shared effects across the various pathologies. In this paper we propose a different approach. We leverage the data collected on multiple

pathologies within each individual in the ROS and MAP studies to identify loci that display pleiotropic effects on multiple pathologies within the same individual and thus influence multiple insults and pathways to neurodegeneration. Such loci could be excellent targets of further investigation both in understanding Tau pathology and in exploring the shared pathways leading to the central nervous system response to different disease processes.

## Methods

### Participants

The subjects consisted of participants from two longitudinal cohort studies operated out of The Rush Alzheimer's Disease Center in Chicago, the Religious Order Study (ROS) and the Rush Memory and Aging Project (MAP). All participants are required to sign an informed consent and an Anatomical Gift Act at enrollment, agreeing to donate their brains (ROS) or brains, spinal cords, and select nerves and muscles (MAP) to the study upon death. Both studies were approved by the Institutional Review Board of Rush University Medical Center.

The ROS and MAP studies are maintained and the data are collected by a single group of researchers at the Rush Alzheimer's Disease Center. Data collectors in both studies are cross-trained to allow efficient merging of data and all analyses are performed on the two cohorts combined. A more comprehensive description of the ROS and MAP studies can be found in previous publications<sup>3, 4</sup>.

At the time of analysis there were over 1,200 deceased participants combined in the ROS and MAP cohorts. Of these, 909 were successfully genotyped, all of whom had non-missing values for all seven pleiotropic phenotypes and covariates: neuritic plaque, neurofibrillary tangles, diffuse plaque, amyloid angiopathy, micro and macro infarct, and Lewy bodies, age at death and sex.

The Adult Changes in Thought (ACT) cohort, used for replication in this analysis, is a community-based study of brain aging and dementia which collects data on neuropathology on a sub-sample of their participants' post-mortem. Participants in ACT are age 65 or older at enrollment, randomly sampled from a multi-center health maintenance organization from King County, Washington. More detailed information on the ACT cohort is published elsewhere<sup>5-7</sup>

### Pathological phenotypes

The neuropathological phenotypes analyzed included: neuritic plaque (NP), neurofibrillary tangles (NFT), diffuse plaque (DP), presence of Lewy bodies, microscopic and gross (macroscopic) infarcts, and cerebral amyloid angiopathy.

For ROS and MAP, brain removal was performed at either Rush University or at one of 12 designated sites across the country and sent to the Rush Alzheimer's Disease Center where all post-mortem data collection occurred. Detailed descriptions of the autopsy procedure are published elsewhere<sup>8-11</sup>. In brief, neuritic plaques (NP), diffuse plaques (DP) and neurofibrillary tangles (NFT) were observed with a modified Bielschowsky silver stain and counted in five regions of the brain: midfrontal, temporal, inferior parietal, entorhinal, and

hippocampus. For each measure in each region, counts were normalized by dividing by the standard deviation, and a z score of the counts within each region was calculated. For the global measure of each AD pathology, we averaged these scores over the 5 regions, followed by a square root transformation which allowed us to treat it as a normally distributed continuous variable<sup>12</sup>. Cerebral amyloid angiopathy (CAA) was evaluated in four neocortical regions of the brain: midfrontal, midtemporal, angular and calcarine cortices. Three monoclonal anti-human  $\beta$ -amyloid antibodies with the following dilutions were used for the assessment: 1) 6F/3D (1:50, Dako North America Inc., Carpinteria, CA), 2) 10D5 (1:600, Elan Pharmaceuticals, San Francisco, CA) and 3) 4G8 (1:9000, Covance Labs, Madison, WI). A score for  $\beta$ -amyloid deposition ranging from 0 (no deposition) to 4 (circumferential deposition in over 75% of vessels in the total region) was determined from meningeal and parenchymal vessels in each region separately, with the final score for the region defined as the maximum score between meningeal and parenchymal CAA scores. Finally, a final CAA score was created using the average score across the four regions in each individual and classified as none, mild, moderate and severe using consistent thresholds determined by the neuropathologist.<sup>13</sup> Lewy bodies present in either the nigra or cortex was defined using consensus guidelines established by the international consortium on dementia with Lewy bodies<sup>14</sup>. Details of microscopic and macroscopic infarct measurements are detailed in previous literature<sup>15</sup>. Briefly, all suspected or visualized gross infarcts were further dissected for histological confirmation. Microscopic infarct measures were taken from examination of a minimum of nine regions in one hemisphere. Both macroscopic and microscopic infarcts were analyzed as binary, presence in at least one region or absence in all regions. Braak staging was performed according to consensus criteria for ROS, MAP and ACT cohorts<sup>16, 17</sup> with detailed methods reported in previously published literature<sup>9, 18</sup>.

## Genotyping

DNA used for genotyping ROS and MAP participants was collected from postmortem brain tissue, whole blood, or lymphocytes. The final QCed dataset consisted of 1709 participants were genotyped on the Affymetrix GeneChip 6.0 platform (Santa Clara, CA, USA) at the Broad Institute's Center for Genotyping or the Translational Genomics Research Institute and 384 were genotyped on the Illumina OmniQuad Express platform at Children's Hospital of Philadelphia, of these 799 and 110, respectively, had pathology information and were included in these analyses. The EIGENSTRAT software was used to calculate principle components used to control for population sub-structure and analysis was limited to only those of European decent.<sup>19</sup> All DNA samples go through the same rigorous quality control process before and after genotype generation, and we see no difference in data quality based on source of DNA. Further information regarding genotyping and imputation can be found in previous publications.<sup>20, 21</sup>

RNA-Seq expression data were generated from frozen dorsolateral prefrontal cortex tissues following the construction of complementary DNA libraries. The paired-end reads were mapped using the Ensemble human genome transcriptomic database (<http://www.ensembl.org>). RNA expression of the associated AD genes was queried and examined for an association with AD pathologies. Details on the RNA-Seq expression profiling are provided in the eMethods in the Supplement.

## Statistical Analysis

We used t-tests and chi squared tests to compare ROS and MAP participants on demographic characteristics and pathological traits

For each of the continuous pathological phenotypes (NP, DP, and NFT) we performed univariate GWAS using linear regression in PLINK. We analyzed dichotomous outcomes (Lewy body dementia and micro and macro infarctions) in PLINK with logistic regression. We used R to analyze an ordinal CAA outcome ([www.r-project.org](http://www.r-project.org)) using ordered logistic regression with the function *polr* from the package *MASS* (Agresti, 2002). To minimize artifacts of imputation, we analyzed samples from the Affymetrix and Illumina platforms independently and then meta-analyzed the findings using a fixed effects method weighting by the inverse of the standard error. We used PLINK to meta-analyze the continuous and dichotomous phenotypes, and METAL to meta-analyze CAA<sup>22</sup>. For the cis-eQTL analysis we used linear regression to assess the association between significant loci from the NFT analyses and mRNA expression within 1 Mb of the analyzed SNP.

We used the *mPhen* function in the R package MultiPhen 2.0 to perform the pleiotropic GWAS<sup>23</sup>. MultiPhen performs an inverted ordered logistic regression with SNP as the outcome and the phenotypes and covariates as the independent variables. The value for SNP used in *mPhen* is the dosage rounded to its nearest integer 0, 1 or 2. A chi-squared test statistic is calculated from the comparison of two models with a likelihood ratio test: one model containing all pleiotropic phenotypes plus covariates against a second model containing only covariates. The p-value is based on the resulting chi-square statistic, where the number of pleiotropic phenotypes equals the number of degrees of freedom.

In the pleiotropy GWAS, we pooled the data and adjusted for platform within the regression. Since the pathology phenotypes are associated with age at death and sex all 8 GWASes, (7 univariate and 1 pleiotropic), were adjusted for age at death, sex, cohort (ROS or MAP) and the first 3 principal components to account for population substructure.<sup>24</sup>

## Results

### Discovery study for susceptibility to NFT accumulation

Characteristics of the participants (n=909 with full data), including means (SD) and frequency (%) of the pathology measures are reported in Table 1. The results of the primary analysis, a GWAS for NFT burden, are presented in Table 2. As expected, we find that the *APOE* locus on chromosome 19 is the top result, consistent with prior studies in this cohort<sup>8</sup> and studies in other populations<sup>2, 25</sup>. The Q-Q and Manhattan plots for the GWAS of NFT burden are presented in Supplemental Figures S1 and S2.

Outside of *APOE*, we find a SNP, rs560380, that exceeds a threshold of genome-wide significance in an intron of *PTPRD* ( $p=3.1 \times 10^{-8}$ ) (Figure 1). The variance explained by the *PTPRD* locus is 3%, which is second only to the *APOE* locus (rs429358) at 9% in terms of contribution to overall variation in NFT burden. We were able to replicate this result (with the same direction of effect) in an independent dataset generated from participants in the Adult Changes in Thought (ACT) study, a longitudinal study of older participants who are



non-demented at enrollment. ACT participants do not have the same quantitative NFT measure, but we find a  $p=0.02$  for association with the  $n=380$  participants (46% male and average age at death of 87.2 years ( $SD=6.4$ )) with a complementary phenotype of the same pathology: Braak stage, a semi-quantitative rating scale based on the topographic progression of NFT. For completeness, we also evaluated the Braak stage in ROS and MAP participants in a secondary analysis, and we find that rs560380 is also associated with the Braak phenotype. Using an ordinal logistic regression analysis we see consistency across the three studies (ROS:  $\beta=0.31$ ,  $p=0.0099$ ; MAP:  $\beta=0.41$ ,  $p=0.0002$ ; ACT:  $\beta=0.30$ ,  $p=0.021$ ,  $\beta$  for each additional “A” (major) allele): together, the three sets of subjects have a meta-analyzed  $p$ -value of  $5.3 \times 10^{-7}$ . As expected, the quantitative NFT burden and Braak stage are strongly correlated (Spearman  $r=0.867$ ) in the ROS and MAP cohorts. Having replicated evidence of association between a variant and NFT, we initiated additional analyses to investigate possible mechanisms of the association.

Besides NFT accumulation, many other neuropathologic traits are assessed in ROS and MAP, which we used to further characterize the impact of the *PTPRD* locus. rs560380 had a nominal association with neuritic plaques (NP;  $\beta=0.07$ ,  $p=0.005$ ). NP are the form of amyloid  $\beta$  plaques most closely associated with AD dementia, and the co-occurrence of NP and NFT neuropathologically characterizes AD. We find that rs560380 was nominally associated with a pathologic diagnosis of AD (OR = 1.27, 95% CI (1.04, 1.55),  $p=0.018$ ). Since amyloid  $\beta$  accumulation is thought to precede the accumulation of NFT in the context of AD<sup>26</sup>, we evaluated whether the *PTPRD* association with NFT was driven by this specific pathophysiologic process. We first performed a mediation analysis that compares a model without NP to one with NP included as a covariate. In the basic model, rs560380 has a beta of 0.10 ( $p=3.8 \times 10^{-8}$ ) for the association with NFT, and, in the model that also includes NP, we see a beta of 0.07 ( $p=1 \times 10^{-6}$ ), a reduction of 33% of the effect size of the SNP. This indicates partial mediation of the SNP's effect by NP accumulation; however, the majority of the SNP's effect is not mediated through NP. Results are similar when using measures of amyloid  $\beta$  and Tau pathology derived from immunohistochemistry as previously reported for *APOE*<sup>27</sup> (data not shown). Consistent with the effect of the *PTPRD* locus being due to more than one pathophysiologic process, we find that rs560380 remains associated with NFT burden in the absence of NP: in the subset of 132 participants with no NP on neuropathologic examination, we find a beta of 0.06 ( $p=0.02$ ), which is similar to the SNP's effect size (beta=0.07) in the analysis adjusting for NP (Figure 2).

We also find modest evidence that rs560380 is also associated with other neuropathologic traits: rs560380 is also weakly associated with cerebral amyloid angiopathy ( $p=0.002$ ), a form of amyloid  $\beta$  vasculopathy. We repeated these analyses adjusting for *APOE*  $\epsilon 4$  burden and with the exception of the *APOE* haplotype, we found no meaningful change in effects sizes or  $p$ -values. (Supplemental Table 1)

We assessed whether the rs560380 variant influences mRNA expression in RNA sequence data available from the dorsolateral prefrontal cortex (DLPFC) of 494 ROS and MAP participants, a subset of our dataset. We did not find evidence that rs560380 or the single SNP in LD (rs324543,  $R^2 > 0.5$ ) had an effect on either the level of *PTPRD* expression or the abundance of its different isoforms in our sample (data not shown). Since these data are

generated from cerebral cortical samples, they do not exclude the possibility that the SNP has effects elsewhere in the CNS: as with many susceptibility variants<sup>28</sup>, its effect may be cell- or context-specific and is simply not appreciated in this particular location and mixture of cells. Further, given that many AD susceptibility alleles influence gene expression in myeloid cells, we also checked expression quantitative trait (eQTL) results generated from healthy participants of the ImmVar project<sup>28</sup>, but we found that the rs560380 variant has no effect on mRNA expression of *PTPRD* in *ex vivo* monocytes or naïve CD4+ T cells. As is standard in cis-eQTL analyses, we examined the expression of all other genes within a 1 Mb radius of the SNP, but *PTPRD* is the only gene found in this genomic segment. Thus, rs560380 does not appear to influence mRNA expression of *PTPRD* in the samples that we have queried to date, and, as is the case for a majority of disease-associated SNPs<sup>28</sup>, its mechanism of action remains unclear.

### Leveraging correlated neuropathologic traits to enhance gene discovery for NFT

Since the participants in the ROS and MAP datasets have information on a wealth of different but related neuropathologic phenotypes, we chose to pursue a complementary strategy for further gene discovery: we implemented a secondary analysis for pleiotropy to identify variants that affect not only NFT but also other neuropathologies. Such pleiotropic effects are likely in the context of neurodegeneration in which different insults may ultimately trigger similar responses in neurons and other CNS cells.

We first calculated a correlation matrix between seven neuropathologic outcomes that are available in almost all of our participants. Results are presented in Supplementary Table 2, showing, as expected, modest to strong correlations between findings, ranging from  $\rho = 0.41$  ( $p < 0.001$ ) between NFT and diffuse amyloid plaques (DP) to 0.69 ( $p < 0.001$ ) between NP and DP. Lewy body pathology was not correlated ( $\rho < 0.1$ ) ( $ps > 0.05$ ) with the other traits, and the two neurovascular pathology traits (microscopic and macroscopic strokes) showed only weak ( $\rho = 0.25$ ,  $p < 0.001$ ) correlation with each other. Thus, the observed level of correlation, while substantial in certain cases, remains within the range in which a pleiotropic analysis can be considered: a prior study showed that, even in the presence of correlations as high as 0.9, the MULTIPHEN method shows no inflation in the type I error<sup>23</sup>.

We therefore used MULTIPHEN to implement a pleiotropy analysis integrating results from association studies of seven neuropathologic traits (see details in the online methods section). The *APOE* locus serves as a positive control since it is known to influence several of these traits<sup>29</sup>. Results are presented in Table 3; Q-Q and Manhattan plots for the MULTIPHEN GWAS are presented in Supplementary Figures S3 and S4. Overall, the most significant SNP in the *APOE* locus is rs429358 ( $p = 2.9 \times 10^{-33}$ ) which is in partial LD with the *APOEε4* haplotype. This variant is strongly associated with 4 of the 7 neuropathologic outcomes (NP,  $p = 3.0 \times 10^{-24}$ ; DP,  $p = 1.3 \times 10^{-20}$ ; NFT,  $p = 4.1 \times 10^{-20}$ , and cerebral amyloid angiopathy (CAA),  $p = 5.2 \times 10^{-25}$ ), but it had no significant association with microscopic infarcts, macroscopic infarcts, or Lewy bodies ( $ps > 0.05$ , results not shown). While our pleiotropy results for rs429358 are similar to what is reported in a recent GWAS of neuropathologic traits<sup>2</sup>, we do not replicate their association with our lewy body measure



( $p=0.46$ , ever vs. none). However we were able to replicate their findings for rs6857 using similar phenotypes; NP as a continuous trait in our analyses ( $p = 6.2 \times 10^{-20}$ ) versus an ordinal train in Beecham ( $3.1 \times 10^{-47}$ ), NFT as a continuous trait in our analyses ( $p = 5.0 \times 10^{-18}$ ) versus an ordinal Braak score in Beecham ( $4.7 \times 10^{-47}$ ), CAA as an ordinal trait in our analyses ( $p = 1.9 \times 10^{-21}$ ) versus binary in Beecham ( $p=2.9 \times 10^{-21}$ ) (Supplementary Table 3).

Looking at the top non-*APOE* results that are not significant but have a  $p < 1 \times 10^{-5}$  in the pleiotropy analysis, we note a few interesting results. First, there are a few examples where a SNP such as rs12597858, near the *HS3ST4* gene, has a modest association with NFT burden ( $p=0.0039$ ) in the primary analysis and a much stronger pleiotropy score ( $p=9.5 \times 10^{-6}$ ) [table 3] that is driven by a broad effect on 5 of the remaining 6 neuropathologic traits: NP burden ( $p=0.003$ ), DP burden ( $p=0.03$ ), Lewy bodies ( $p=0.03$ ), CAA ( $p=0.03$ ) and macroscopic infarcts ( $p=0.0003$ ) (Figure 3). *HS3ST4* encodes a protein involved in heparan sulfate biosynthesis. Notably, heparan sulfate proteoglycans have been implicated in many different biological and pathologic processes, including AD and the cellular propagation of both Tau and  $\alpha$ -synuclein pathologies<sup>30–32</sup>. Another example of a SNP whose effect becomes appreciable only when considering multiple neuropathologic traits is in the *POLD3* gene: the top SNP, rs4145953 has a modest effect on NFT burden ( $p=2.4 \times 10^{-4}$ ) and a stronger pleiotropic score ( $p=1.1 \times 10^{-6}$ ) (Table 3), which is driven by additional, modest associations with NP burden ( $p=1.1 \times 10^{-4}$ ), DP burden ( $p=2.7 \times 10^{-5}$ ) and macroscopic infarcts ( $p=0.01$ ).

As compared to *HS3ST4* whose pleiotropic association is driven by a modest effect on many neuropathologies, a second type of locus, like *PTPRD*, has a strong effect on one trait and modest effects in 2 other traits: NP ( $p=0.005$ ) and cerebral amyloid angiopathy ( $p=0.002$ ). Thus, not surprisingly, this SNP is suggestive but not significant in the pleiotropy analysis ( $p=9.7 \times 10^{-6}$ ), with this association being driven primarily by the NFT trait. In another example, SNP chr3:197113961 in the *SLC29A4* gene is nearly significant genome-wide in the pleiotropic analysis ( $p=6.6 \times 10^{-8}$ ) and is driven by effects on microscopic ( $p=3.4 \times 10^{-6}$ ) and macroscopic ( $p=9.3 \times 10^{-4}$ ) infarcts. However, this variant has no effects on non-vascular traits.

Tables with the top results for the GWAS for all the neuropathologies examined are presented in Supplementary Tables S4 – S9, and QQ plots and Manhattan plots for each trait are presented in Supplementary Figures S5–S16.

### Role of known disease-associated variants in NFT accumulation and pleiotropy

We also evaluated more closely the role of SNPs known to be associated with tauopathies (AD and PSP)<sup>25, 33</sup>. Results are displayed in Table 4. In the 24 susceptibility loci that we evaluate<sup>33–36</sup>, we found a significant NFT association (using a significance cut-off of  $0.002=0.05/24$ ) with the rs1476679 SNP in the *ZCWPWI* locus ( $\beta=0.07$ ,  $p=4.9 \times 10^{-4}$ ) (Table 4). As with the *PTPRD* variant, rs1476679 also influences NP ( $p=0.0043$ ), and, when we adjust for NP, the beta of the NFT association ( $\beta=0.037$ ,  $p=0.024$ ) was reduced by 47%. Thus, in this case, much of the SNP's effect appears to be mediated through pathologic processes that underlie NP. The only other locus to show some level of suggestive

association with NFT in our data is rs10948363, a SNP in the *CD2AP* gene ( $p = 0.0085$ ), consistent with a recent report and our earlier results<sup>2, 37</sup>.

Since both *ZCWPW1* and *CD2AP* are known AD susceptibility loci, we tested if this association is mediated through NFT pathology. In our data only the *ZCWPW1* SNP (rs1476679) is associated with AD risk ( $\beta = 0.32$ ,  $p=0.003$ ), and the effect is attenuated 50% with the addition of NFT ( $\beta = 0.15$ ,  $p=0.23$ ). No SNPs in *CD2AP* were associated with AD risk in our limited dataset.

## Discussion

Our primary analysis reports a significant association between the *PTPRD* locus and the accumulation of NFT in older participants. While the detailed molecular mechanism of this association remains unclear at present, we find that the effect of the rs560380 SNP on NFT accumulation is not dependent on a single pathophysiologic process. NP mediates part of the SNP's effect on NFT, but most of the effect is independent of NP, and the association is observed in individuals without substantial amyloid  $\beta$  pathology. This pattern of findings suggests that rs560380 may be a locus that influences the central nervous system's response to different insults that can lead to neuronal dysfunction and neurodegeneration.

*PTPRD* is a large gene that has previously been associated with restless leg syndrome (RLS)<sup>38–40</sup> and, less convincingly, obsessive compulsive disorder (OCD)<sup>41</sup>. The SNPs driving these associations are not found on the same susceptibility haplotype as the NFT-associated *PTPRD* variant and suggest the presence of allelic heterogeneity and phenotypic heterogeneity: *PTPRD* is implicated in NFT accumulation as well as neurologic disorders without Tau pathology. The SNPs associated with OCD and RLS – two conditions that are not tauopathies – do not display an association with NFT burden in our data (data not shown). In terms of tauopathies, an existing PSP GWAS does not provide evidence of significant association with *PTPRD*. In terms of AD, a suggestive association of *PTPRD* with AD dementia susceptibility has been reported previously ( $p=4.5 \times 10^{-5}$ )<sup>36</sup> in one AD GWAS and in our own data, we see a modest association with AD dementia susceptibility ( $p=0.04$ , with clinical diagnosis of AD dementia). Overall, further studies are needed to evaluate the extent of the role of this locus to clinical manifestations associated with the accumulation of NFT. Our evidence to date highlights a role for *PTPRD* in the accumulation of this pathologic feature, irrespective of its clinical manifestations.

*PTPRD* encodes the protein tyrosine phosphatase receptor-type delta protein, which is reported to have protein tyrosine phosphatase activity *in vitro*<sup>42</sup>. It is expressed in the brain where it has been implicated in synaptic differentiation<sup>43</sup>. A null allele in mice leads to memory impairment and altered electrophysiological responses in the hippocampus<sup>44</sup>. Further, in our prior work, *PTPRD* was considered among other AD candidate genes for studies using a *Drosophila* model, and knockdown of *lar*, the fly orthologue of *PTPRD*, was discovered to enhance Tau-induced retinal degeneration, consistent with its association with NFT accumulation in humans<sup>45</sup>. Further work in flies and other model systems is now necessary to delineate the molecular consequences of perturbations in *PTPRD* expression that lead to Tau pathology.

Aside from *PTPRD*, we note that the validated AD susceptibility *ZCWPW1* allele has a significant effect on NFT accumulation (Figure 2). However, unlike *PTPRD*, the effect of this variant appears to be mediated more strongly through an effect on amyloid  $\beta$  accumulation.

The other locus that deserves some discussion is *HS3ST4*, which had a modest effect of NFT burden but a strongly suggestive association in the pleiotropy analysis because of its effect on 6 of the 7 available neuropathologic measures. This association was also supported by our earlier work in *Drosophila*: the homolog of another gene encoding a heparan sulfate biosynthetic enzyme, *HS6ST3*, influenced Tau toxicity in a *Drosophila* transgenic model<sup>46</sup>. This result is consistent with the emerging potential role of heparan sulfate proteoglycans as receptors for the spread of Tau and synuclein pathologies<sup>47</sup>. Notably, variants at loci encoding other heparan sulfate sulfotransferases have been strongly suggested in AD (*HS3ST1*, rs448799,  $p=6.6\times10^{-8}$ )<sup>33</sup> as well as a study of memory performance in non-demented individuals (*HS3ST4*, rs11074779  $p=3.1\times10^{-8}$ )<sup>48</sup>.

In comparing our study to the recently published GWAS of multiple neuropathologies<sup>2</sup>, we showed similar findings with the *APOE* region being associated with the NFT, NP and CAA outcomes plus a strong pleiotropic association, however were unable to replicate their novel findings. This discordance can be explained by the multiple differences between the two studies, specifically, differences in phenotype definitions and sample selection since our subjects come from prospective studies of aging and are not recruited in specialty dementia clinics.

Our study of older participants has certain limitations, including the fact that participants are non-demented at study entry, biasing us towards a population of older individuals that have survived to an advanced age without dementia. On the other hand, we have the advantage of performing all autopsies using a single structured protocol at a single site, minimizing phenotypic error. In contrast to the recent study that also performed a GWAS for NFT by repurposing genotypes generated for an AD study<sup>2</sup>, our participants were not originally selected to fit certain clinicopathologic criteria. Since such a selection of AD “cases” and “controls” will influence the distribution of pathology and may limit the generalizability of its results, it was not pursued here. These features and the moderate sample sizes used in this study and the earlier NFT GWAS of AD cases and controls<sup>25</sup> could explain differences in the results of the two studies. However, we do have similar findings with the *APOE* region: we find it to be associated with the NFT, NP and CAA outcomes, but we were unable to replicate the novel finding of association with Lewy bodies. We note that the present study has high internal validity as follow-up rates exceeded 95% and autopsy rates exceeded 90% and the limited power due to small sample size should not detract from the positive results that meet reasonable thresholds of statistical significance.

In sum, this NFT GWAS begins to uncover genetic variation that influences the accumulation of Tau pathology in older individuals. In addition, we present evidence supporting the utility of a pleiotropic analysis approach in identifying genetic variation with shared effects in common brain pathologies. These two approaches - focused and pleiotropic

- are complementary and will both be necessary to dissect the complex web of inter-related factors that lead impaired cognition and, ultimately, dementing syndromes.

## Supplementary Material

Refer to Web version on PubMed Central for supplementary material.

## Acknowledgments

We thank all the participants of the Religious Orders Study the Rush Memory and Aging Project and the Adult Changes in Thought, as well as the staff at the Rush Alzheimer's Disease Center for this work. This work was supported by the National Institutes of Health [grants P30AG10161, R01AG15819, R01AG17917, R01AG36042, R01AG36836, K25AG041906 and U01AG46152]

## References

1. Johnson VE, Stewart W, Smith DH. Widespread Tau and Amyloid-Beta Pathology Many Years After a Single Traumatic Brain Injury in Humans. *Brain Pathol.* 2012; 22(2):142–149. [PubMed: 21714827]
2. Beecham GW, Hamilton K, Naj AC, Martin ER, Huentelman M, Myers AJ, et al. Genome-wide association meta-analysis of neuropathologic features of Alzheimer's disease and related dementias. *PLoS genetics.* 2014; 10(9):e1004606. [PubMed: 25188341]
3. Bennett DA, Schneider JA, Arvanitakis Z, Wilson RS. Overview and findings from the religious orders study. *Curr Alzheimer Res.* 2012; 9(6):628–645. [PubMed: 22471860]
4. Bennett DA, Schneider JA, Buchman AS, Barnes LL, Boyle PA, Wilson RS. Overview and findings from the rush Memory and Aging Project. *Curr Alzheimer Res.* 2012; 9(6):646–663. [PubMed: 22471867]
5. Kukull WA, Higdon R, Bowen JD, McCormick WC, Teri L, Schellenberg GD, et al. Dementia and Alzheimer disease incidence: a prospective cohort study. *Arch Neurol.* 2002; 59(11):1737–1746. [PubMed: 12433261]
6. Sonnen JA, Larson EB, Haneuse S, Woltjer R, Li G, Crane PK, et al. Neuropathology in the adult changes in thought study: a review. *Journal of Alzheimer's disease: JAD.* 2009; 18(3):703–711. [PubMed: 19661627]
7. Sonnen JA, Larson EB, Crane PK, Haneuse S, Li G, Schellenberg GD, et al. Pathological correlates of dementia in a longitudinal, population-based sample of aging. *Ann Neurol.* 2007; 62(4):406–413. [PubMed: 17879383]
8. Bennett DA, De Jager PL, Leurgans SE, Schneider JA. Neuropathologic intermediate phenotypes enhance association to Alzheimer susceptibility alleles. *Neurology.* 2009; 72(17):1495–1503. [PubMed: 19398704]
9. Bennett DA, Schneider JA, Arvanitakis Z, Kelly JF, Aggarwal NT, Shah RC, et al. Neuropathology of older persons without cognitive impairment from two community-based studies. *Neurology.* 2006; 66(12):1837–1844. [PubMed: 16801647]
10. Bennett DA, Wilson RS, Schneider JA, Evans DA, Beckett LA, Aggarwal NT, et al. Natural history of mild cognitive impairment in older persons. *Neurology.* 2002; 59(2):198–205. [PubMed: 12136057]
11. Bennett DA, Wilson RS, Schneider JA, Bienias JL, Arnold SE. Cerebral infarctions and the relationship of depression symptoms to level of cognitive functioning in older persons. *Am J Geriatr Psychiatry.* 2004; 12(2):211–219. [PubMed: 15010350]
12. Barnes LL, Schneider JA, Boyle PA, Bienias JL, Bennett DA. Memory complaints are related to Alzheimer disease pathology in older persons. *Neurology.* 2006; 67(9):1581–1585. [PubMed: 17101887]
13. Yu L, Boyle PA, Nag S, Leurgans S, Buchman AS, Wilson RS, et al. APOE and cerebral amyloid angiopathy in community-dwelling older persons. *Neurobiology of aging.* 2015

14. McKeith IG, Galasko D, Kosaka K, Perry EK, Dickson DW, Hansen LA, et al. Consensus guidelines for the clinical and pathologic diagnosis of dementia with Lewy bodies (DLB): report of the consortium on DLB international workshop. *Neurology*. 1996; 47(5):1113–1124. [PubMed: 8909416]
15. Arvanitakis Z, Leurgans SE, Barnes LL, Bennett DA, Schneider JA. Microinfarct pathology, dementia, and cognitive systems. *Stroke*. 2011; 42(3):722–727. [PubMed: 21212395]
16. Braak H, Braak E. Neuropathological staging of Alzheimer-related changes. *Acta Neuropathol*. 1991; 82(4):239–259. [PubMed: 1759558]
17. Braak H, Alafuzoff I, Arzberger T, Kretschmar H, Del Tredici K. Staging of Alzheimer disease-associated neurofibrillary pathology using paraffin sections and immunocytochemistry. *Acta neuropathologica*. 2006; 112(4):389–404. [PubMed: 16906426]
18. Sonnen JA, Larson EB, Crane PK, Haneuse S, Li G, Schellenberg GD, et al. Pathological correlates of dementia in a longitudinal, population-based sample of aging. *Annals of neurology*. 2007; 62(4):406–413. [PubMed: 17879383]
19. Price AL, Patterson NJ, Plenge RM, Weinblatt ME, Shadick NA, Reich D. Principal components analysis corrects for stratification in genome-wide association studies. *Nature genetics*. 2006; 38(8):904–909. [PubMed: 16862161]
20. Shulman JM, Chen K, Keenan BT, Chibnik LB, Fleisher A, Thiyyagura P, et al. Genetic susceptibility for Alzheimer disease neuritic plaque pathology. *JAMA Neurol*. 2013; 70(9):1150–1157. [PubMed: 23836404]
21. De Jager PL, Shulman JM, Chibnik LB, Keenan BT, Raj T, Wilson RS, et al. A genome-wide scan for common variants affecting the rate of age-related cognitive decline. *Neurobiol Aging*. 2012; 33(5):1017.e1011–1015.
22. Willer CJ, Li Y, Abecasis GR. METAL: fast and efficient meta-analysis of genomewide association scans. *Bioinformatics*. 2010; 26(17):2190–2191. [PubMed: 20616382]
23. O'Reilly PF, Hoggart CJ, Pomyen Y, Calboli FC, Elliott P, Jarvelin MR, et al. MultiPhen: joint model of multiple phenotypes can increase discovery in GWAS. *PloS one*. 2012; 7(5):e34861. [PubMed: 22567092]
24. Price AL, Patterson NJ, Plenge RM, Weinblatt ME, Shadick NA, Reich D. Principal components analysis corrects for stratification in genome-wide association studies. *Nat Genet*. 2006; 38(8): 904–909. [PubMed: 16862161]
25. Cruchaga C, Kauwe JS, Harari O, Jin SC, Cai Y, Karch CM, et al. GWAS of cerebrospinal fluid tau levels identifies risk variants for Alzheimer's disease. *Neuron*. 2013; 78(2):256–268. [PubMed: 23562540]
26. Jack CR Jr, Knopman DS, Jagust WJ, Shaw LM, Aisen PS, Weiner MW, et al. Hypothetical model of dynamic biomarkers of the Alzheimer's pathological cascade. *The Lancet Neurology*. 2010; 9(1):119–128. [PubMed: 20083042]
27. Bennett DA, Schneider JA, Wilson RS, Bienias JL, Berry-Kravis E, Arnold SE. Amyloid mediates the association of apolipoprotein E e4 allele to cognitive function in older people. *J Neurol Neurosurg Psychiatry*. 2005; 76(9):1194–1199. [PubMed: 16107349]
28. Raj T, Rothamel K, Mostafavi S, Ye C, Lee MN, Replogle JM, et al. Polarization of the effects of autoimmune and neurodegenerative risk alleles in leukocytes. *Science*. 2014; 344(6183):519–523. [PubMed: 24786080]
29. Bennett DA, Wilson RS, Schneider JA, Evans DA, Aggarwal NT, Arnold SE, et al. Apolipoprotein E epsilon4 allele, AD pathology, and the clinical expression of Alzheimer's disease. *Neurology*. 2003; 60(2):246–252. [PubMed: 12552039]
30. Snow AD, Mar H, Nochlin D, Kimata K, Kato M, Suzuki S, et al. The presence of heparan sulfate proteoglycans in the neuritic plaques and congophilic angiopathy in Alzheimer's disease. *Am J Pathol*. 1988; 133(3):456–463. [PubMed: 2974240]
31. Perry G, Siedlak SL, Richey P, Kawai M, Cras P, Kalara RN, et al. Association of heparan sulfate proteoglycan with the neurofibrillary tangles of Alzheimer's disease. *J Neurosci*. 1991; 11(11): 3679–3683. [PubMed: 1941102]

32. van Horssen J, Wesseling P, van den Heuvel LP, de Waal RM, Verbeek MM. Heparan sulphate proteoglycans in Alzheimer's disease and amyloid-related disorders. *The Lancet Neurology*. 2003; 2(8):482–492. [PubMed: 12878436]
33. Lambert JC, Ibrahim-Verbaas CA, Harold D, Naj AC, Sims R, Bellenguez C, et al. Meta-analysis of 74,046 individuals identifies 11 new susceptibility loci for Alzheimer's disease. *Nat Genet*. 2013; 45(12):1452–1458. [PubMed: 24162737]
34. Lambert JC, Heath S, Even G, Campion D, Sleegers K, Hiltunen M, et al. Genome-wide association study identifies variants at CLU and CR1 associated with Alzheimer's disease. *Nat Genet*. 2009; 41(10):1094–1099. [PubMed: 19734903]
35. Hollingworth P, Harold D, Sims R, Gerrish A, Lambert JC, Carrasquillo MM, et al. Common variants at ABCA7, MS4A6A/MS4A4E, EPHA1, CD33 and CD2AP are associated with Alzheimer's disease. *Nat Genet*. 2011; 43(5):429–435. [PubMed: 21460840]
36. Naj AC, Jun G, Beecham GW, Wang LS, Vardarajan BN, Buross J, et al. Common variants at MS4A4/MS4A6E, CD2AP, CD33 and EPHA1 are associated with late-onset Alzheimer's disease. *Nat Genet*. 2011; 43(5):436–441. [PubMed: 21460841]
37. Shulman JM, Imboywa S, Giagtzoglou N, Powers MP, Hu Y, Devenport D, et al. Functional screening in *Drosophila* identifies Alzheimer's disease susceptibility genes and implicates Tau-mediated mechanisms. *Hum Mol Genet*. 2013
38. Yang Q, Li L, Yang R, Shen GQ, Chen Q, Foldvary-Schaefer N, et al. Family-based and population-based association studies validate PTPRD as a risk factor for restless legs syndrome. *Mov Disord*. 2011; 26(3):516–519. [PubMed: 21264940]
39. Schormair B, Kemlink D, Roeske D, Eckstein G, Xiong L, Lichtner P, et al. PTPRD (protein tyrosine phosphatase receptor type delta) is associated with restless legs syndrome. *Nat Genet*. 2008; 40(8):946–948. [PubMed: 18660810]
40. Winkelmann J, Czamara D, Schormair B, Knauf F, Schulte EC, Trenkwalder C, et al. Genome-wide association study identifies novel restless legs syndrome susceptibility loci on 2p14 and 16q12. 1. *PLoS genetics*. 2011; 7(7):e1002171. [PubMed: 21779176]
41. Mattheisen M, Samuels JF, Wang Y, Greenberg BD, Fyer AJ, McCracken JT, et al. Genome-wide association study in obsessive-compulsive disorder: results from the OCGAS. *Mol Psychiatry*. 2014
42. Krueger NX, Streuli M, Saito H. Structural diversity and evolution of human receptor-like protein tyrosine phosphatases. *EMBO J*. 1990; 9(10):3241–3252. [PubMed: 2170109]
43. Takahashi H, Craig AM. Protein tyrosine phosphatases PTPdelta, PTPsigma, and LAR: presynaptic hubs for synapse organization. *Trends Neurosci*. 2013; 36(9):522–534. [PubMed: 23835198]
44. Uetani N, Kato K, Ogura H, Mizuno K, Kawano K, Mikoshiba K, et al. Impaired learning with enhanced hippocampal long-term potentiation in PTPdelta-deficient mice. *EMBO J*. 2000; 19(12):2775–2785. [PubMed: 10856223]
45. The National Institute on Aging, and Reagan Institute Working Group on Diagnostic Criteria for the Neuropathological Assessment of Alzheimer's Disease. Consensus recommendations for the postmortem diagnosis of Alzheimer's disease. *Neurobiol Aging*. 1997; 18(4 Suppl):S1–2. [PubMed: 9330978]
46. Shulman JM, Chipendo P, Chibnik LB, Aubin C, Tran D, Keenan BT, et al. Functional screening of Alzheimer pathology genome-wide association signals in *Drosophila*. *Am J Hum Genet*. 2011; 88(2):232–238. [PubMed: 21295279]
47. Holmes BB, DeVos SL, Kfoury N, Li M, Jacks R, Yanamandra K, et al. Heparan sulfate proteoglycans mediate internalization and propagation of specific proteopathic seeds. *Proceedings of the National Academy of Sciences*. 2013; 110(33):E3138–E3147.
48. DeBette S, Ibrahim Verbaas CA, Bressler J, Schuur M, Smith A, Bis JC, et al. Genome-wide Studies of Verbal Declarative Memory in Nondemented Older People: The Cohorts for Heart and Aging Research in Genomic Epidemiology Consortium. *Biol Psychiatry*. 2015; 77(8):749–763. [PubMed: 25648963]



49. Hoglinger GU, Melhem NM, Dickson DW, Sleiman PM, Wang LS, Klei L, et al. Identification of common variants influencing risk of the tauopathy progressive supranuclear palsy. *Nat Genet.* 2011; 43(7):699–705. [PubMed: 21685912]

# Neurofibrillary Tangles

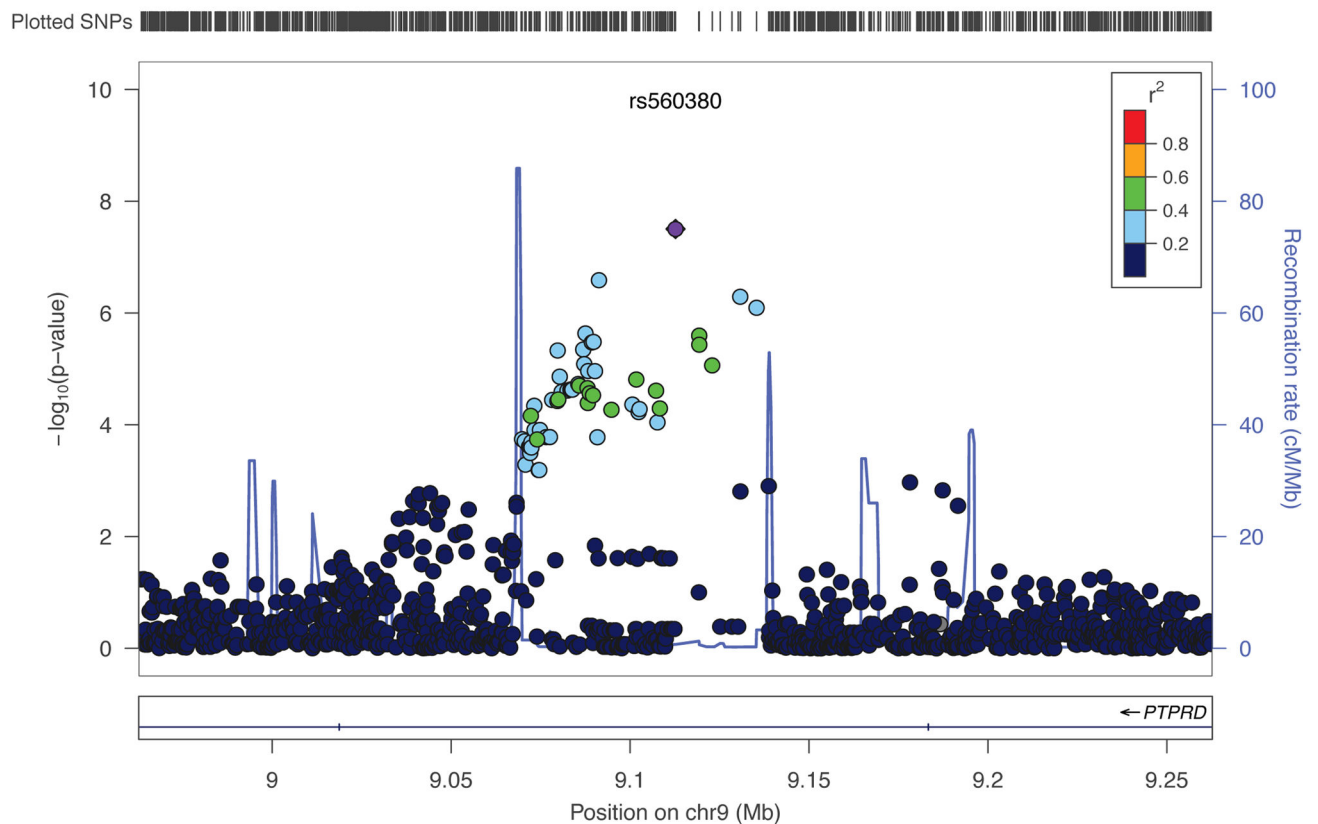


**Figure 1. Regional association plot for *PTPRD* and Neurofibrillary Tangles (NFT)**

The x-axis is the base pair position and the y-axis is the  $-\log(p\text{-value})$  for the association with NFT. The blue line represents the recombination rate.

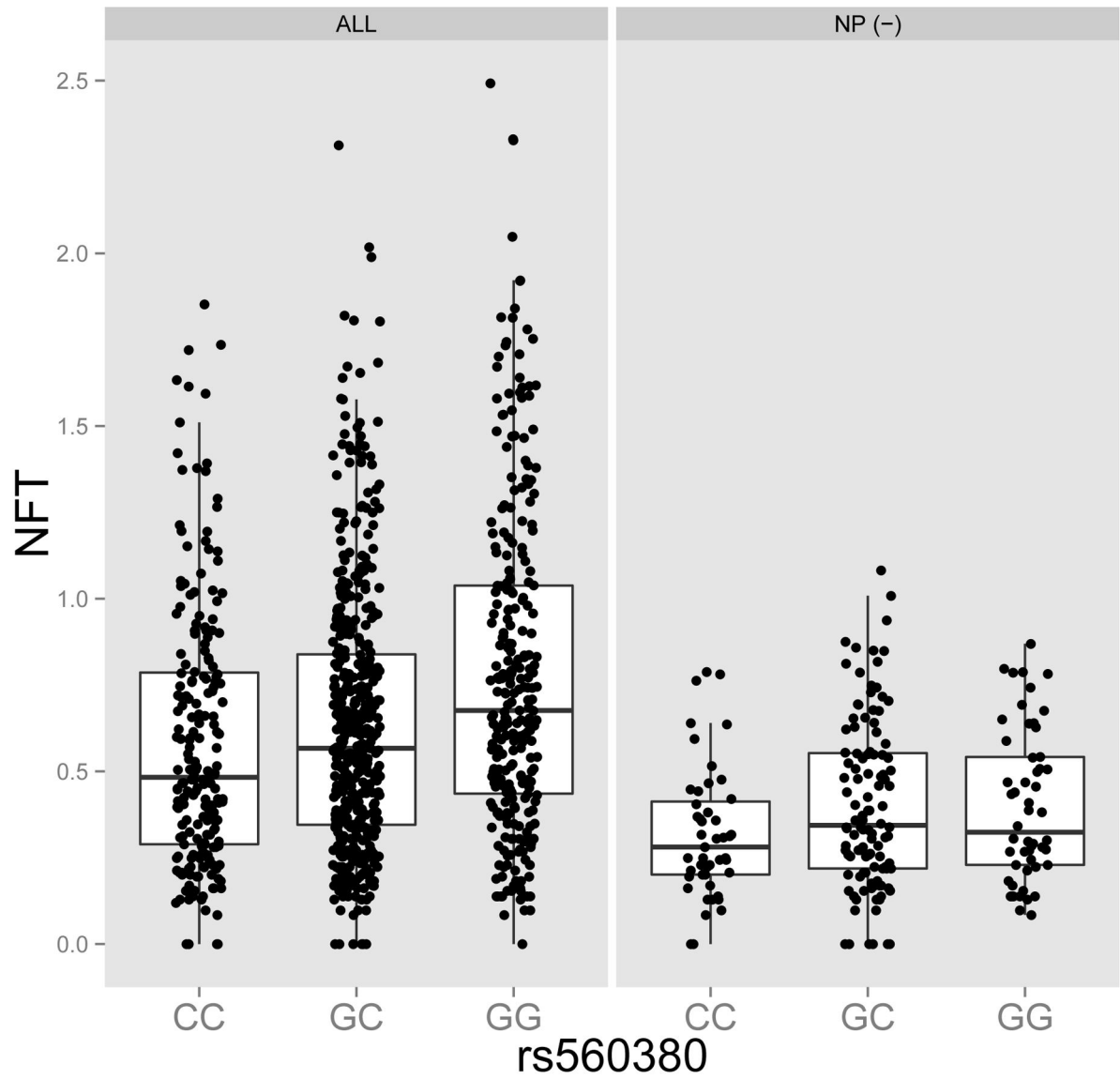


**Figure 2. Association between *PTPRD* SNP, rs560380 and Neurofibrillary Tangles**

The left plot includes all n=909 ROS and MAP brains and the right plot includes a subset of n=132 from participants with no neuritic plaques at death.

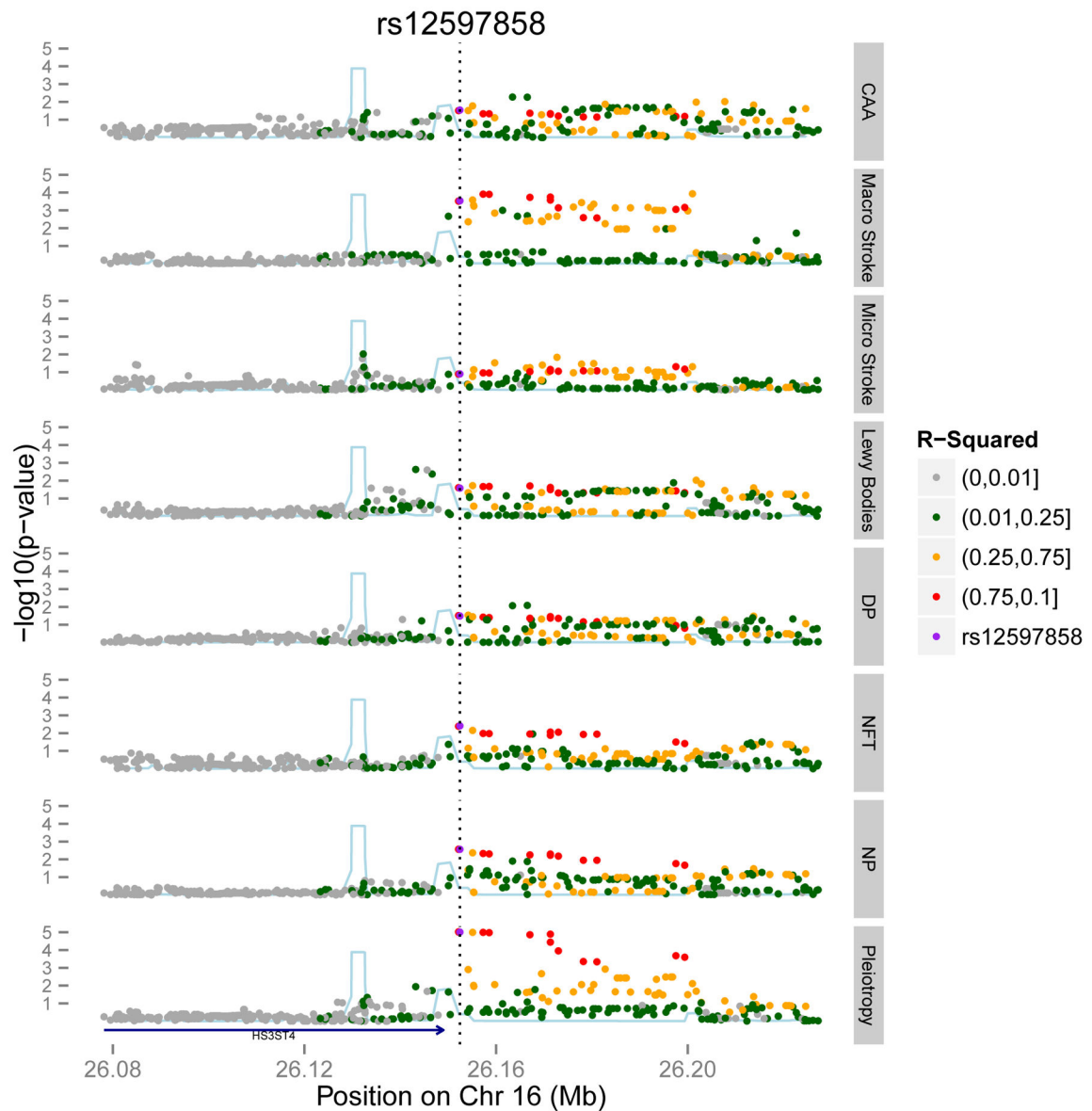


**Figure 3. Regional association plot for *HS3ST4*.**

The x-axis is the base pair position centered around the top pleiotropy snp, rs12597858 and the y-axis is the  $-\log(p\text{-value})$ . The blue line represents the recombination rate. The bottom level shows the pleiotropic results and the top level show results for each of the seven neuropsychological phenotypes.

**Table 1**

Characteristics of the ROS and MAP participants included in analyses

Variable	MAP n=438	ROS n=471	p-value
age at death	89.4 ± (5.8)	87.5 ± (6.9)	<.0001
Male	151 (34%)	174 (37%)	0.480
Pathology dx of AD *	275 (63%)	295 (63%)	>0.99
<b>Pathology</b>			
Lewy Body	87 (20%)	108 (23%)	0.296
Neurofibrillary Tangles	0.70 ± (0.41)	0.66 ± (0.41)	0.171
Neuritic Plaque	0.74 ± (0.53)	0.74 ± (0.54)	0.993
Diffuse Plaque	0.64 ± (0.48)	0.71 ± (0.50)	0.029
Micro Infarct	113 (26%)	140 (30%)	0.213
Macro Infarct	162 (37%)	165 (35%)	0.586
CAA **			0.272
None	78 (18%)	105 (22%)	
Mild	204 (47%)	200 (42%)	
Moderate	105 (24%)	104 (22%)	
Severe	51 (12%)	62 (13%)	

\* NIA-Reagan Criteria,

\*\* CAA - Cerebral Amyloid Angiopathy

Table 2

Significant ( $p < 5.0 \times 10^{-8}$ ) and suggestive ( $p < 1 \times 10^{-5}$ ) results from the GWAS of neurofibrillary tangles

SNP	CHR	BP	Nearest Gene*	region	A1	A2	AF**	OR (95%CI)	p-value
rs429358	19	45411941	<i>APOE/TOMM40</i>	intronic	T	C	0.85	-0.27 (-0.21, -0.33)	4.06E-20
rs560380	9	9112698	<i>PTPRD</i>	intronic	A	C	0.55	0.10 (0.07, 0.14)	3.14E-08
rs2446485	6	21140299	<i>CDKALI</i>	intronic	G	A	0.82	-0.13 (-0.08, -0.17)	1.82E-07
rs9739162	12	1838008	<i>ADIPOR2</i>	intronic	G	T	0.46	-0.09 (-0.05, -0.12)	2.56E-06
rs2104198	20	16653076	<i>SNRNPB2</i>	intergenic	C	T	0.50	-0.08 (-0.05, -0.12)	4.88E-06
rs2964044	5	173720716		intergenic	A	T	0.89	-0.13 (-0.08, -0.19)	5.50E-06
rs11022147	11	1341815	<i>TOLLIP</i>	intergenic	G	A	0.93	-0.25 (-0.14, -0.36)	5.50E-06
chr5:167502615	5	167502615	<i>ODZ2</i>	intronic	T	C	0.97	-0.26 (-0.15, -0.37)	5.85E-06
rs11743956	5	6292456	<i>FLJ33360</i>	intergenic	C	T	0.91	-0.20 (-0.11, -0.28)	6.40E-06
rs12609752	19	56448708	<i>NLRP13</i>	intergenic	C	T	0.98	-0.30 (-0.17, -0.44)	6.52E-06
rs13425639	2	184588957		intergenic	G	A	0.82	-0.11 (-0.06, -0.16)	6.57E-06
rs1494971	8	108650188		intergenic	T	C	0.83	-0.15 (-0.09, -0.22)	6.72E-06
rs10025919	4	146242907		intergenic	T	C	0.88	0.16 (0.09, 0.23)	7.25E-06
chr6:53236216	6	53236216	<i>ELOVL5</i>	intergenic	A	G	0.94	-0.26 (-0.14, -0.37)	7.80E-06
rs73035809	11	131606984	<i>NTM</i>	intronic	G	A	0.97	-0.39 (-0.22, -0.56)	8.18E-06
chr3:98769677	3	98769677		intergenic	T	C	0.91	-0.21 (-0.12, -0.3)	9.63E-06
rs73183521	8	2955118	<i>CSMD1</i>	intronic	T	C	0.98	-0.42 (-0.23, -0.6)	1.01E-05

\* Within 100 kb of SNP;

\*\* Allele frequency of A1



**Table 3**

Significant ( $p < 5.0 \times 10^{-8}$ ) and suggestive ( $p < 1 \times 10^{-5}$ ) results from pleiotropic analyses.

SNP	CHR	BP	Nearest Gene*	region	A1	A2	AF**	P
rs429358	19	45411941	<i>APOE/TOMM40</i>	intronic	T	C	0.85	2.88E-33
chr3:197113961	3	197113961	<i>LOC100507086</i>	intergenic	C	G	0.96	6.60E-08
chr15:41258121	15	41258121	<i>CHAC1</i>	intergenic	C	T	0.96	1.02E-06
rs4145953	11	74331879	<i>POLD3</i>	intronic	A	G	0.80	1.07E-06
chr6:44535225	6	44535225			G	T	0.95	1.18E-06
rs2291354	15	25952889	<i>ATP10A</i>	intronic	A	G	0.48	1.23E-06
rs11584308	1	14805993			C	G	0.80	1.46E-06
rs72723271	4	188308255	<i>LOC339975</i>	intronic	T	G	0.94	1.63E-06
rs2446485	6	21140299	<i>CDKAL1</i>	intronic	G	A	0.82	2.18E-06
rs59008350	20	18219685	<i>ZNF133/CSRP2BP</i>	intergenic	C	T	0.96	2.21E-06
rs11765038	7	5336105	<i>SLC29A4</i>	intronic	A	G	0.32	3.55E-06
chr3:70929100	3	70929100	<i>FOXP1</i>	intergenic	G	T	0.91	4.97E-06
rs7107464	11	36584944	<i>RAG1</i>	intergenic	T	C	0.91	4.98E-06
rs6540796	1	213821667			A	G	0.70	5.45E-06
rs9321429	6	134475749	<i>SGK1</i>	intergenic	C	G	0.64	5.50E-06
chr1:245947879	1	245947879	<i>SMYD3</i>	intronic	A	C	0.99	6.52E-06
rs10836184	11	34325250	<i>ABTB2</i>	intronic	T	C	0.21	6.68E-06
rs348147	8	73353197			G	A	0.89	7.27E-06
rs66657970	11	134377829	<i>LOC283177</i>	intergenic	C	T	0.97	8.60E-06
rs7206188	16	26152155	<i>HS3ST4</i>	intergenic	T	C	0.56	9.45E-06
rs12142743	1	146585620	<i>PRKAB2</i>	intergenic	G	T	0.89	9.66E-06
rs560380	9	9112698	<i>PTPRD</i>	intronic	A	C	0.55	9.92E-06

\* Within 100 kb of SNP;

\*\* Allele frequency of A1

**Table 4**

Associations of known AD and PSP SNPs with the neurofibrillary tangles and pleiotropic outcomes.

Gene	Chr	SNP	POS	Allele Frequency	p-value (NFT)	p-value (pleiotropy)
<b>Significant SNPs from AD GWAS*</b>						
<i>CR1</i>	1	rs6656401	207692049	0.815	0.2771	0.3152
<i>BIN1</i>	2	rs7561528	127889637	0.655	0.6676	0.1816
<i>BIN1</i>	2	rs6733839	127892810	0.397	0.2380	0.2190
<i>INPP5D</i>	2	rs35349669	234068476	0.463	0.1829	0.7458
<i>MEF2C</i>	5	rs190982	88223420	0.407	0.2733	0.8914
<i>CD2AP</i>	6	rs10948363	47487762	0.256	<b>0.0086</b>	<b>0.0284</b>
<i>TREM2</i>	6	rs9381040	41154650	0.279	0.2548	0.0695
<i>HLA-DRB5</i>	6	rs9271192	32578530	0.708	0.2342	0.8329
<i>ZCWPW1</i>	7	rs1476679	100004446	0.707	<b>0.0005</b>	<b>0.0308</b>
<i>NME8</i>	7	rs2718058	37841534	0.636	0.6656	0.1890
<i>EPHA1</i>	7	rs11771145	143110762	0.641	0.1856	0.8026
<i>CLU</i>	8	rs9331896	27467686	0.403	0.3164	0.4114
<i>PTK2B</i>	8	rs28834970	27195121	0.349	0.6440	0.4197
<i>CELF1</i>	11	rs10838725	47557871	0.694	0.8936	0.0501
<i>PICALM</i>	11	rs10792832	85867875	0.364	0.1130	0.5884
<i>SORL1</i>	11	rs11218343	121435587	0.969	0.5155	0.6918
<i>MS4A6A</i>	11	rs983392	59923508	0.572	0.5211	0.6942
<i>FERMT2</i>	14	rs17125944	53400629	0.912	0.0852	0.0145
<i>SLC24A4</i>	14	rs10498633	92926952	0.775	0.1696	0.5026
<i>DSG2</i>	18	rs8093731		0.006	MAF < 1%, No results	
<i>APOE</i>	19	rs4420638	45422946	0.827	<b>1.85E-14</b>	<b>2.29E-26</b>
<i>APOE</i>	19	rs2075650	45395619	0.863	<b>5.90E-14</b>	<b>9.45E-23</b>
<i>ABCA7</i>	19	rs4148929	73740837	0.609	0.9686	0.1547
<i>CD33</i>	19	rs3865444	51727962	0.689	0.8673	0.4297
<i>CASS4</i>	20	rs7274581	55018260	0.919	0.9493	0.5211
<b>Significant SNPs from PSP GWAS**</b>						

Gene	Chr	SNP	POS	Allele Frequency	p-value (NFT)	p-value (pleiotropy)
<i>STX6</i>	1	rs1411478	179229155	0.391	0.9068	0.7213
<i>EIF2AK3</i>	2	rs7571971	88676716	0.266	0.0851	0.4059
<i>MOBP</i>	3	rs1768208	39498257	0.706	0.3310	0.3190
<i>MAPT</i>	17	rs8070723	41436651	0.202	0.7335	0.4593
<i>MAPT</i>	17	rs242557	41375823	0.620	0.9564	0.4059

\* Lambert, et. al *Nat Gen* 2013<sup>33</sup>, Hoglinger, et. al. *Nat Gen* 2011<sup>49</sup>